

# APPLICATION OF CONTROLLED SOURCE AUDIO MAGNETOTELLURIC (CSAMT) AT GEOTHERMAL

Susilawati<sup>1\*</sup>, Enjang Jaenal Mustopa<sup>2</sup>

<sup>1</sup>*Department of Informatics, Computer Science Faculty, Singaperbangsa Karawang University  
Jl. H.S. Ronggowaluyo, East Karawang 41361*

<sup>2</sup>*Department of Physics, Mathematic and Natural Science of Faculty, Institute Technology of  
Bandung  
Jl. Ganeca no. 10 Bandung*

Received: 21<sup>th</sup> March 2017; Revised: 27<sup>th</sup> April 2017; Accepted: 30<sup>th</sup> April 2017

## ABSTRACT

CSAMT or Controlled Source Audio-Magnetotelluric is one of the Geophysics methods to determine the resistivity of rock under earth surface. CSAMT method utilizes artificial stream and injected into the ground, the frequency of artificial sources ranging from 0.1 Hz to 10 kHz, CSAMT data source effect correction is inverted. From the inversion results showed that there is a layer having resistivity values ranged between 2.5  $\Omega$ .m – 15  $\Omega$ .m, which is interpreted that the layer is clay.

**Keywords:** CSAMT; resistivity; clay

## Introduction

CSAMT method is a geophysical method which can be applied to search for natural resources such as minerals, geothermal, oil and gas. CSAMT method is a development method of MT (Magnetotelluric) method. In CSAMT method, using artificial sources by injecting electric current can control and minimize noise or interference that comes from nature. CSAMT method is very effective for mapping resistivity contrasts of rock below the surface to a depth of 2-3 km.<sup>1</sup> However, due to using artificial sources, the primary waves recorded by a receiver which is necessary to effect correction source. The CSAMT method is used to identify areas with massive sulfide anomalies as the main targets due to their conductive properties. The CSAMT method has been successfully applied for gold exploration in Washington, USA, the CSAMT method also successfully mapped uranium exploration. The CSAMT method is also successful for mapping of resistivity at geothermal, Takigami in Kyushu.<sup>2</sup>

In this paper, Horizontal Electric Dipole (HED) was modeled to study the response of the distance between transmitter and receiver. The comparison of field data correction source effect is the main result to run the inversion using Non-Linear Conjugate Gradient (NLCG) inversion.

The geothermal system in Indonesia is divided into two categories, vapor domination system, and hot water domination system. The Kamojang geothermal system proved that the vapor domination system with reservoir temperature between 230°C until 246°C with the depth of reservoir above 800 m – 1300m.<sup>3</sup>

As scheme the structure of the geothermal system as the figure 1. The top zone is a conductive zone (smectite) with the temperature of 70°C. At the higher temperature, illite from the less conductive layer become the mix layer illite-smectite. The proportion of illite increase with the rise of temperature become 180°C. The smectite temperature is decreased and the pure illite appears at the higher temperatures from

\*Author Corresponding:

E-Mail: susilawati.sobur@staff.unsika.ac.id

220°C.<sup>4</sup> The target of the geothermal system has low resistivity. The low of resistivity is the top of reservoir.<sup>5</sup>

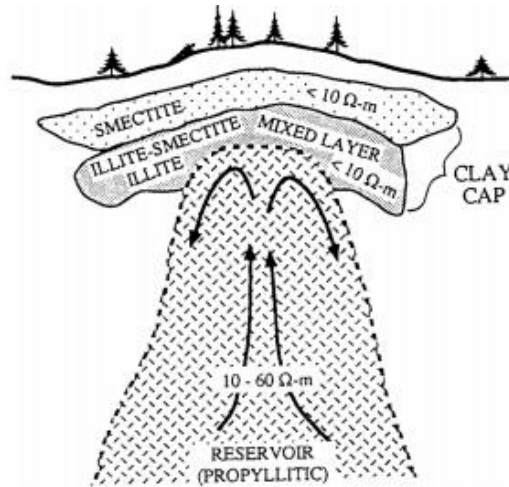


Figure 1. The geothermal system scheme.<sup>4</sup>

**Methods**

The modeling used the concept of Horizontal Electric Dipole (HED) where the impedance depends on the field intensity which is caused the source dipole with long dx in cylinder coordinate and the dipole current is sinusoidal. The distance r from the source of horizontal, the intensity field which measuring on the surface with the attention to the Maxwell equation and the field intensity to the potential vector will get related like that.<sup>6</sup>

$$H_r = -\frac{Idx}{2\pi r} \sin \phi \left\{ \frac{1}{2} \int_0^\infty J_1(mr) dm + \frac{r}{2} \int_0^\infty m J_0(mr) dm \right\} = -\frac{Idx}{4\pi r^2} \sin \phi \quad (1)$$

$$H_\phi = \frac{Idx}{2\pi r} \cos \phi \int_0^\infty J_1(mr) dm = \frac{Idx}{4\pi r^2} \cos \phi \quad (2)$$

$$H_z = \frac{Idx}{4\pi r} \sin \phi \int_0^\infty m J_1(mr) dm = \frac{Idx}{4\pi r^2} \sin \phi \quad (3)$$

$$E_r = \frac{\rho_1 dx}{\gamma \pi} \cos \phi \left[ -\int_0^\infty \frac{m^2}{R_o} J_0(mr) dm + \frac{1}{r} \int_0^\infty \frac{m}{R_o} J_1(mr) dm \right] \quad (4)$$

with

$$R_o = \coth \left[ mH_1 + \coth^{-1} \left( \frac{\rho_1}{\rho_2} \right) \coth \left\{ mH_2 + \coth^{-1} \left( \frac{\rho_{N-1}}{\rho_N} \right) \right\} \right] \quad (5)$$

The apparent resistivity at the far field is:

$$\rho_a^f = \frac{1}{\mu \omega} |Z|^2 \quad (6)$$

$$\rho_a^f = \frac{1}{\mu \omega} |Z|^2$$

With replace  $\mu$  and  $\omega = 2\pi f$ , and the conversion unit, so we get:

$$\rho_a = \frac{1}{5f} \left| \frac{E_\phi}{H_r} \right|^2 \Omega.m. \quad (7)$$

$$\rho_a^f = \frac{1}{\mu \omega} |Z|^2$$

$$\rho_a = \frac{K_f}{5f} \left| \frac{E_\phi}{H_r} \right|^2 \Omega.m. \quad (8)$$

$$\rho_a^f = \frac{1}{\mu \omega} |Z|^2$$

The apparent resistivity at the near field is

$$\rho_a^n = \frac{rZ_n}{2} \quad (9)$$

$$Z_n = \frac{2\rho}{r} \quad \rho_a^f = \frac{1}{\mu \omega} |Z|^2$$

$$\rho_a^n = K_n r \left| \frac{E_\phi}{H_r} \right|^2 \Omega.m. \quad (10)$$

$$\rho_a^f = \frac{1}{\mu \omega} |Z|^2$$

The formula for determining the far resistivity value and the near resistivity value as follows:

$$\rho_a^f = \frac{1}{\mu \omega} |Z|^2 \quad \rho_a^f = \frac{K_f}{5f} \left| \frac{E_x}{H_y} \right|^2 \Omega.m. \quad (11)$$

$$\rho_a^f = \frac{1}{\mu \omega} |Z|^2 = K_n r \left| \frac{E_x}{H_y} \right|^2 \Omega.m. \quad (12)$$

### Result and Discussion

HED modeling was conducted in three layers where the first layer is 100 Ω.m with the thickness 100 meter. Resistivity value at second layer is 10 Ω.m with thickness is 50 meter And the third layer has resistivity value 50Ω.m. The modeling is done with the distance between transmitter and receiver is different.

There are three data on each graph, the first line is blue color presenting the resistivity to the frequency in the far field calculated using equation (11), the second data is resistivity to the frequency in near field calculated using equation (12) and the third graph is resistivity to a frequency with

corrected source effect. The Triangle transition zone was formed by a correction in the transition zone. Once the low frequency, the value of skin depth runs high, To reach the far field zone, it's required a great distance, then for the area that is less than 4δ conducted the correction, so for the low frequency is used the apparent resistivity equation of near field and for high frequencies used far field. The below is a survey map of Kamojang geothermal field. a survey was conducted by using CSAMT with 60 points of sounding, measurement data consists of 7 lines, there are *line 1, line 2, line 3, line 4, line 5 and line 6.*

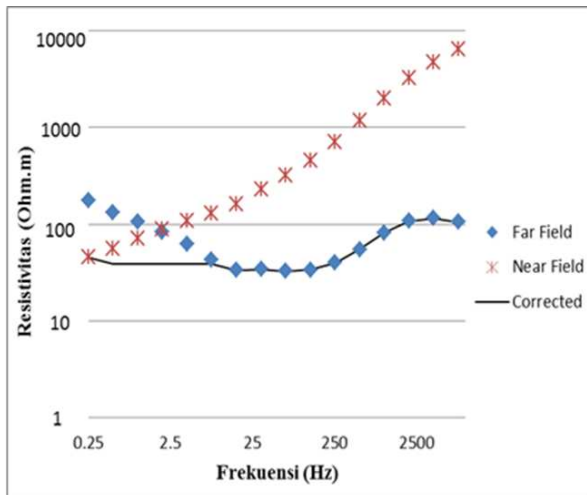


Figure 2a. HED modeling with the distance is 4.4 km.

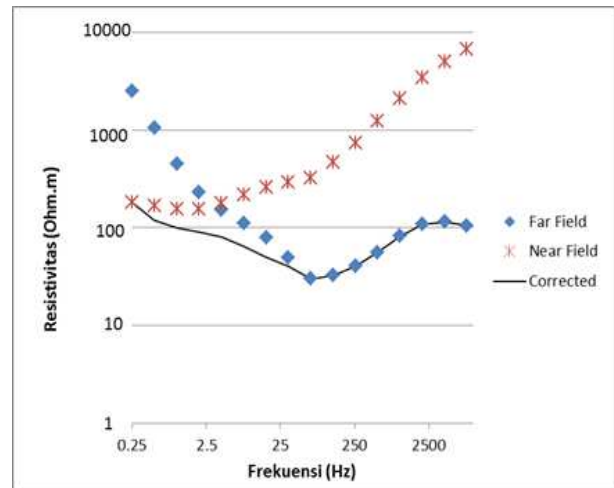


Figure 2 c. HED modeling with the distance is 1.8 km.

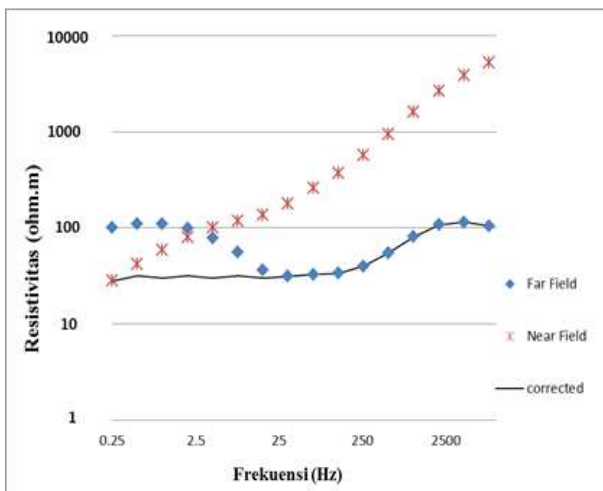


Figure 2 b. HED modeling with the distance is 3.6 km

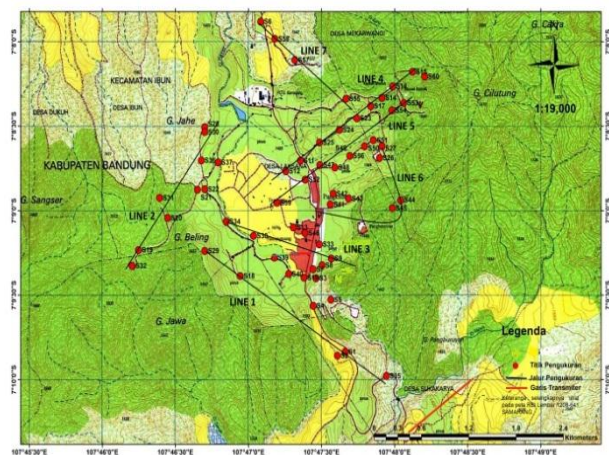
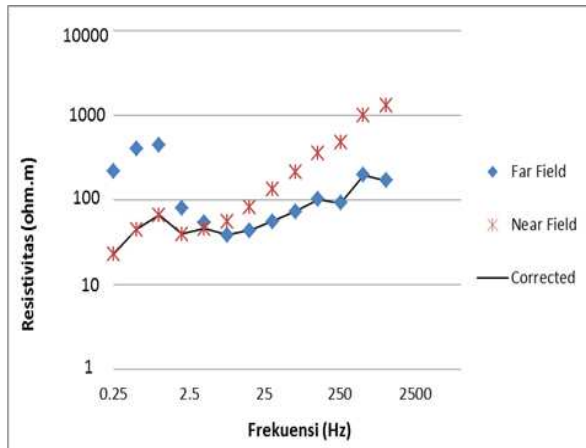


Figure 3. CSAMT survey map on the Kamojang field.

The results of correction source effect at sounding-1 and sounding-57 with a distance

transmitter and receiver are different.



**Figure 4a.** The correction result of sounding 1 (distance 1.34 km)

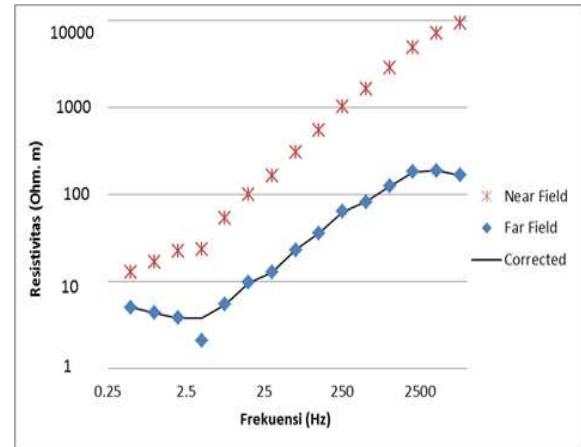


**Figure 4b.** The correction result of sounding 57 (distance 4.22 km)

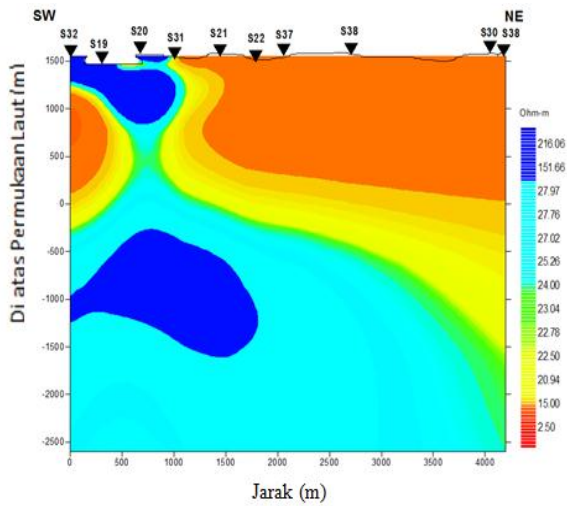


**Figure 5a.** Line 1

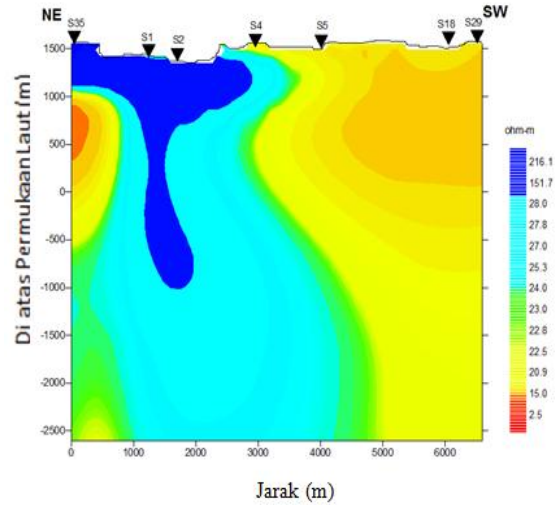


**Figure 5b.** Line 2

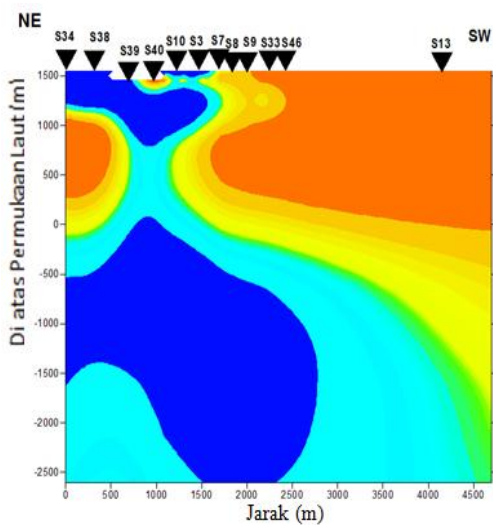


**Figure 5c.** Line 3

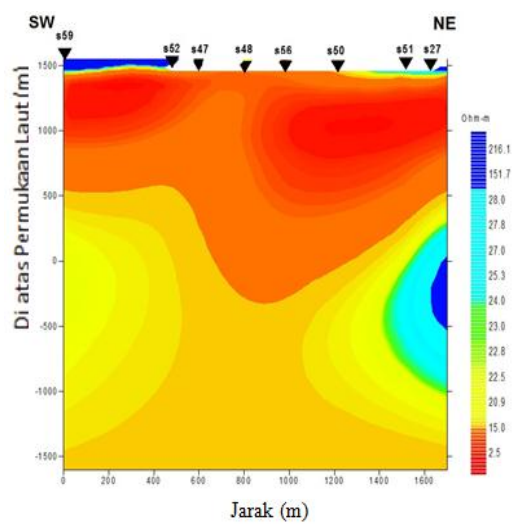


**Figure 5d.** Line 4

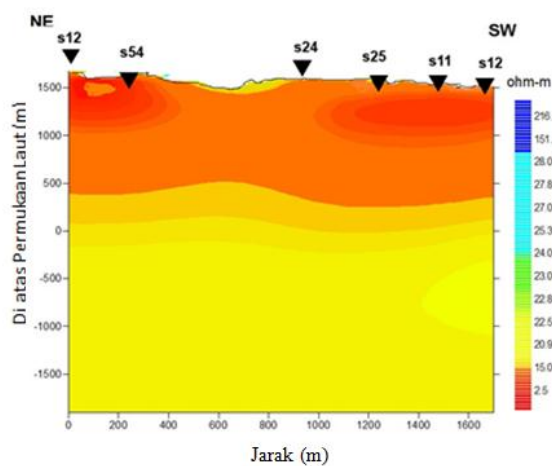


Figure 5e. Line 5

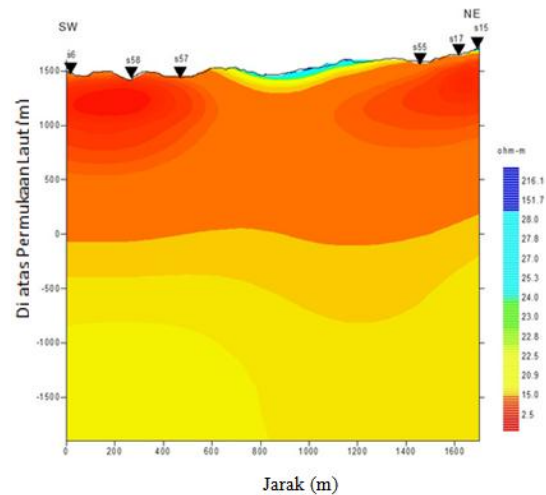


Figure 5f. Line 6

All soundings did the inversion after did the source effect correction, the inversion is used that are Non-Linear Conjugate Gradients (NLCG).<sup>6</sup>

In the figure 5.a that is the inversion result at line 1, SW direction on the first layer there is a layer with resistivity values ranging from 15 to 22.5  $\Omega$ .m, and in the direction of NE on the first layer has a very high resistivity values are above 100  $\Omega$ .m, at line 1 there are no layers with low resistivity values, so we interpretation that the first line there is no reservoir. The results inversion on line 2, line 3, line 4, line 5 and line 6. Each of which is shown in the figure 5.b, 5.c 5.d, 5.e and 5.f the range of resistivity value are 2.5-15  $\Omega$ .m and below that layer, there is a layer with higher resistivity values and below that layer, there is a layer with higher resistivity values. Then interpreted that these layers are clay as the covering layer.

### Conclusion

CSAMT method can be used to detect the geothermal reservoir area by detecting the value of resistivity at each layer. Based on the value of resistivity, it interpreted that the first line there is no reservoir due to the absence of layers with low resistivity values. While on line 2, line 3, line 4, line 5 and line 6 there are low resistivity values ranged

between 2.5-15  $\Omega$ .m interpreted as clay layer covering layer.

### References

1. Zonge, K. L., and Hughes, L. J., Controlled Source Audio-Frequency Magnetotellurics.1991.
2. Mustopa et al. Resistivity Structure in Kamojang Geothermal Field Derived from CSAMT Data: Indonesian Journal of Physics. 2011. Vol.11, No.1.
3. Saptadji, M., N., (2009). Karakterisasi reservoir panas bumi, Training “Advanced Geothermal Reservoir Engineering, 6-17 Juli. Institut Teknologi Bandung, Jl. Ganesa 10 Bandung, Indonesia.
4. Johnston, J.M., Pellerin, L. and Hohmann, G.W., Evaluation of Electromagnetic Methods for Geothermal Reservoir Detection. Geothermal Resources Council Transactions, 1992. Vol 16. pp 241 – 245.
5. Ussher, G., et al. 2000. Understanding The Resistivities Observed In Geothermal Systems. Proceedings World Geothermal Congress.
6. Kaufman, A.A., Keller, G.V., Frequency and Transient Soundings, Elsevier, Amsterdam. 1983. p.685.
7. Rodi, W., Mackie, R. L., Nonlinear conjugate gradients algorithm for 2-D magnetotelluric inversion. Geophysics. 2001. 66, 174-187.